Journal of the European Ceramic Society **11** (1993) 115–122

Relations Between Composition and Microstructure of Sialons

G. Z. Cao, R. Metselaar

Centre for Technical Ceramics, Eindhoven University of Technology, PO Box 513, 5600 MB Eindhoven, The Netherlands

&

G. Ziegler

Institute for Materials Research, Bayreuth University, 8580 Bayreuth, Germany

(Received 24 March 1992; accepted 7 July 1992)

Abstract

The relationship between composition and microstructure of sialon ceramics was studied. Fully dense yttrium-containing α′- and α′ + β′-sialon ceramics were prepared by gas pressure sintering. Additionally, the effect of La_2O_3 as a sintering additive was investigated. Experimental results reveal that the typical microstructure of these sialon ceramics consists of a crystalline phase of sialon(s) and a small fraction of amorphous phase remaining at grain boundaries. The composition of the amorphous phase is very similar, both in α′- and α′ + β′-sialon ceramics. However, the amount of the amorphous phase increases with increasing amount of oxides used in the starting mixtures. The α′- and α′ + β′-sialons exhibit differences in grain size and grain morphology. The addition of La_2O_3 to the starting mixtures promotes the incorporation of yttrium ions into the crystal lattice and leads to the formation of crystal defects in the α′-grains.

Es wurde der Zusammenhang zwischen Zusammensetzung und Gefüge von Sialon-Keramiken untersucht. Vollständig verdichtete Yttrium-haltige α′ + β′-Sialon-Keramiken wurden durch Gasdrucksintern hergestellt. Des weiteren wurde der Einfluß von La_2O_3 als Sinteradditiv untersucht. Die experimentellen Ergebnisse zeigen, daß ein typisches Gefüge dieser Sialon-Keramiken aus einer kristallinen Sialon-Phase und einem geringen Anteil verbleibender amorpher Phase an den Korngrenzen besteht. Die Zusammensetzung der amorphen Phase ist sehr einheitlich, sowohl in α′- als auch in α′ + β′-Sialon-Keramiken. Der Anteil an amorpher Phase nimmt jedoch mit steigendem Anteil an Oxiden in den Ausgangsmischungen zu. Die α′- und α′ + β′-Sialone weisen Unterschiede in Korngröße und -morphologie auf. Der Zusatz von La_2O_3 zu den Ausgangsmischungen beschleunigt das Eindringen der Yttriumionen in das Kristallgitter und führt zur Bildung von Kristalldefekten innerhalb der α′-Körner.

Les auteurs ont étudié la relation entre la composition et la microstructure de céramiques en sialon. Des céramiques tout-à-fait denses en sialon α′ et α′ + β′ contenant de l'yttrium ont été préparées par frittage sous pression gazeuse (GPS). De plus, l'effet de La_2O_3 en tant qu'additif de frittage a été examiné. Les résultats expérimentaux montrent que la microstructure typique de ces sialons consiste en une phase cristalline en sialon et en une petite fraction de phase amorphe localisée aux joints de grains. Dans les deux cas examinés (α′ et α′ + β′), la composition de la phase amorphe est très semblable. Cependant, sa quantité augmente avec la quantité d'oxydes présents dans le mélange de départ. Les sialons α′ et α′ + β′ se distinguent par leur taille et leur morphologie des grains. L'addition de La_2O_3 dans la composition initiale favorise l'incorporation des ions yttrium dans le réseau cristallin et conduit à la formation de défauts cristallins dans les grains α′.

1 Introduction

The α′- and/or mixed α′ + β′-sialon ceramics have attracted attention both as cutting tools and as potential materials used at high temperatures and in corrosive environments. In this respect it is important that α′-sialons offer the possibility to incorporate the sintering aids, like yttria, into the lattice[1,2] and

Journal of the European Ceramic Society 0955-2219/93/$6.00

thus enhance the chemical and mechanical properties, especially at high temperatures. It is proposed that by combination of careful processing and heat treatment the amount of glassy grain boundary phase can be kept very low[3] or can be fully crystallized.[4] It has also been shown that advanced sintering techniques such as gas pressure sintering and hot isostatic pressing can be used successfully to obtain fully dense sialon ceramics.[5-8] In the present study the relationship between the amount and composition of oxide additive(s) and the microstructure of the final sialon ceramics is discussed.

Cations, such as La^{3+} or Ce^{3+}, are considered to be too large to be incorporated into the crystal lattice,[1-3] but it has been shown that as sintering additives for silicon nitride and/or sialon ceramics they can improve the sinterability and mechanical properties.[9-11] Thus, La_2O_3 as an extra sintering additive was used for improving the formation of sialon and the final densification, and modifying the composition of the glassy grain boundary phase. Recently Olsson[12] and Ekström *et al.*[13] reported that Ce^{3+} cations (radius 1·034 Å) can enter the lattice of α′-sialons. Thus, it is also of interest to see whether La^{3+} cations (radius 1·061 Å), together with Y^{3+} (radius 0·892 Å) are soluble too.

2 Experimental Procedure

The starting materials used in the present investigation were Si_3N_4 (LC-12, Starck, Berlin, Germany, with 1·57 wt% oxygen), AlN (Grade C, Starck, with 1·80 wt% oxygen), Al_2O_3 (CR 10, Baikalox (Baikowski Chimie, Annecy, France), 99·99 wt%), Y_2O_3 (Ventron (Karlsruhe, Germany), 99·99 wt%) and La_2O_3 (Fluka AG (Buchs, Switzerland), 99·99 wt%). The chemical composition of the starting mixtures as well as the phase compositions α′/β′ and the densities of the final products are presented in Table 1. The oxygen impurity in the nitrides was not taken into account. The powders were mixed by ball milling in ethanol for 50 h with hot-pressed silicon nitride (HPSN) balls. After drying, the mixtures were pressed uniaxially at 1 MPa, and then isostatically under 250 MPa. Specimens were 25 mm in diameter and 7 mm in thickness.

The specimens, embedded in a mixture of 75 wt% silicon nitride, 20 wt% aluminium nitride and 5 wt% yttria, were sintered in a gas pressure furnace first at 1800°C for 60 min under a nitrogen pressure of 0·5 MPa, followed by 1900°C for 30 min under 10 MPa N_2. Fully dense sialon ceramics (relative density not less than 99·8 th.%) were obtained; the overall weight loss was about 1 wt%.

The microstructural analysis was performed by means of XRD, SEM and TEM (with energy-dispersive spectrometry (EDS)) observation. For SEM observations, polished specimens were etched by using Plasma Enhanced CVD under the following conditions: temperature 300°C, pressure 600 mtorr, 300 kHz, 100 W for 10 min with mixed CF_4/O_2 (5 vol%) with a flow rate of 200 ml/min. In addition, fracture surfaces were studied by SEM. The TEM specimens were cut to thin foils of about 20 μm, then ion milled and coated with carbon. Besides imaging, the selected area diffraction technique was used to determine the different phases. The amount of secondary phase was calculated from TEM micrographs.

3 SEM Observations

Figure 1 gives the SEM fractograph of α′-sialon sample A. It is seen that α′-sialon has a homogeneous microstructure with equi-axed grains with mean grain size of approximately 4 μm. A very similar microstructure was found in the case of sample C which contained 2·53 wt% alumina in the starting mixtures. However, the addition of La_2O_3 to the starting mixture (sample E) leads to a much finer-grained microstructure with a mean grain size of only 2 μm (see Fig. 2), nearly a factor 2 smaller than that of sample A.

Figure 3 presents the back scattered electron micrograph of the polished surface of sample B. The dark bars are β′-phase, the white spots identify the amorphous phase at grain boundaries, while the matrix consists of α′-sialon. Figure 4 shows the

Table 1. The chemical composition of the starting mixtures and the phase composition and density of the final products

Specimen	*Mixture (wt%)*					*Final products*	
	Si_3N_4	*AlN*	Y_2O_3	Al_2O_3	La_2O_3	α′/(α′ + β′)	*Density* (g/cm^3)
A	75·41	15·25	9·34	0	0	1	3·29
B	87·37	7·83	4·80	0	0	0·75	3·23
C	72·10	16·04	9·33	2·53	0	1	3·28
D	80·92	9·76	4·79	4·83	0	0·35	3·23
E	71·82	14·52	8·90	0	4·76	1	3·35

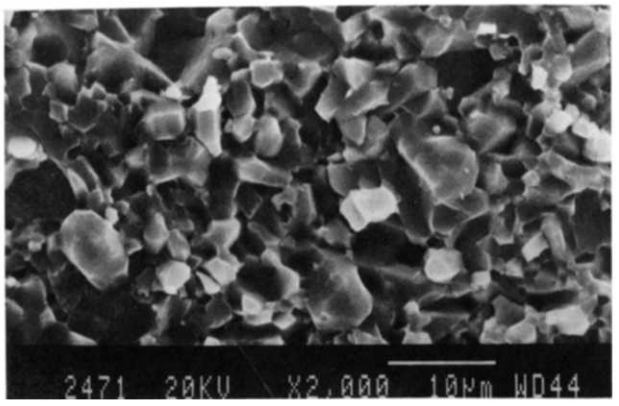

Fig. 1. SEM fractograph of α'-sialon sample A. The bar is 10 μm.

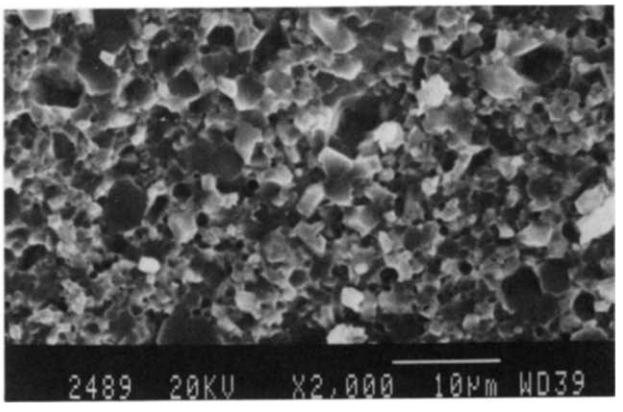

Fig. 2. SEM fractograph of α'-sialon sample E containing La_2O_3. The bar is 10 μm.

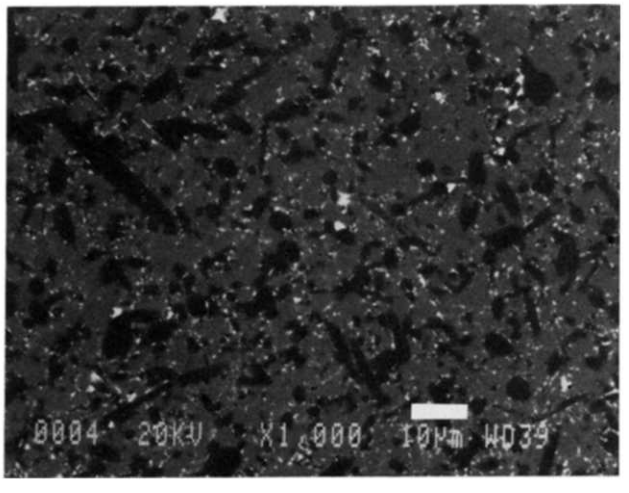

Fig. 3. The back scattered electron micrograph of the polished and etched surface of the $\alpha' + \beta'$ composite sample B. The bar is 10 μm.

typical fracture surface of the mixed $\alpha' + \beta'$-sialon ceramics with $\alpha'/(\alpha' + \beta') \approx 0{\cdot}75$ (sample B). It is seen that there are two types of grains: the equi-axed grains with a mean grain size of 3 μm are α'-phase, like in monolithic α'-sialon ceramics, and the needle- or fibre-like grains are β'-phase with an aspect ratio of about 7. For the β'-phase grains an average length of about 14 μm and a width of about 2 μm were observed. In contrast to the monolithic α'-sialon

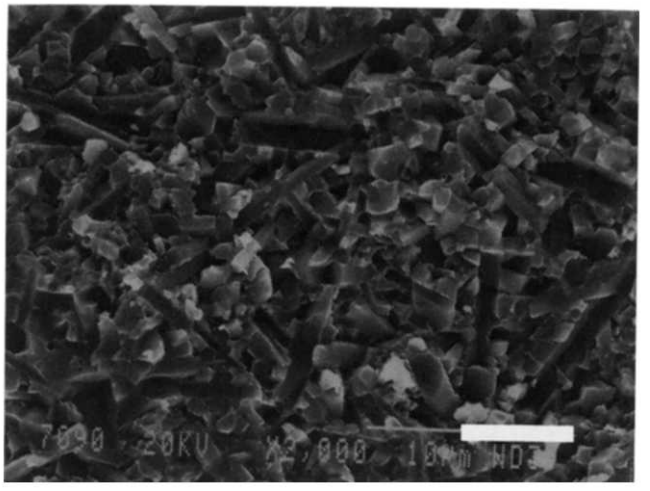

Fig. 4. SEM fractograph of mixed $\alpha' + \beta'$-sialon sample B. The bar is 10 μm.

ceramics, the addition of alumina powder to the starting mixture of the α'–β' composites results in a decrease of the aspect ratio of the β'-sialon grains. In sample D, with $\alpha'/(\alpha' + B') \approx 0{\cdot}35$, an aspect ratio of about 4 was obtained with grains of 10 μm in length and about 2·5 μm in width, while the morphology and the grain size of the α'-phase remains almost the same.

4 TEM Observations

TEM imaging together with EDS analysis and selected-area electron diffraction technique, was applied for the study of the amount and the composition of the grain boundary phase of these sialon ceramics.

Figure 5 shows the TEM microphotograph of α'-sialon ceramics (sample A). Only one crystalline phase, the α'-sialon, was detected. Sample A contains approximately 8·5 vol% of an amorphous phase, which is present not only at the intersections of three and four grains, but also between two grains. This implies that all crystal grains are covered with a thin film of amorphous material. The EDS analysis indicates that the amorphous phase at grain boundaries is rich in yttrium and aluminium with an atom ratio Si:Al:Y = 1:0·6:0·8. This is different from the average content in the overall composition of the sample, Si:Al:Y = 1:0·23:0·05.

Figure 6 shows the TEM microphotograph of the mixed $\alpha' + \beta'$-sialon sample B. Similar to specimen A with only monolithic α'-sialon, a glassy phase is always observed at grain boundaries, although the amount of grain boundary amorphous phase, about 3·5 vol% in sample B, is much smaller. Furthermore, the composition of the glassy phase, in atom ratio Si:Al:Y = 1:0·5:0·8, in comparison with the overall composition Si:Al:Y = 1:0·10:0·02, appears quite similar to that in the α'-sialon material A. However,

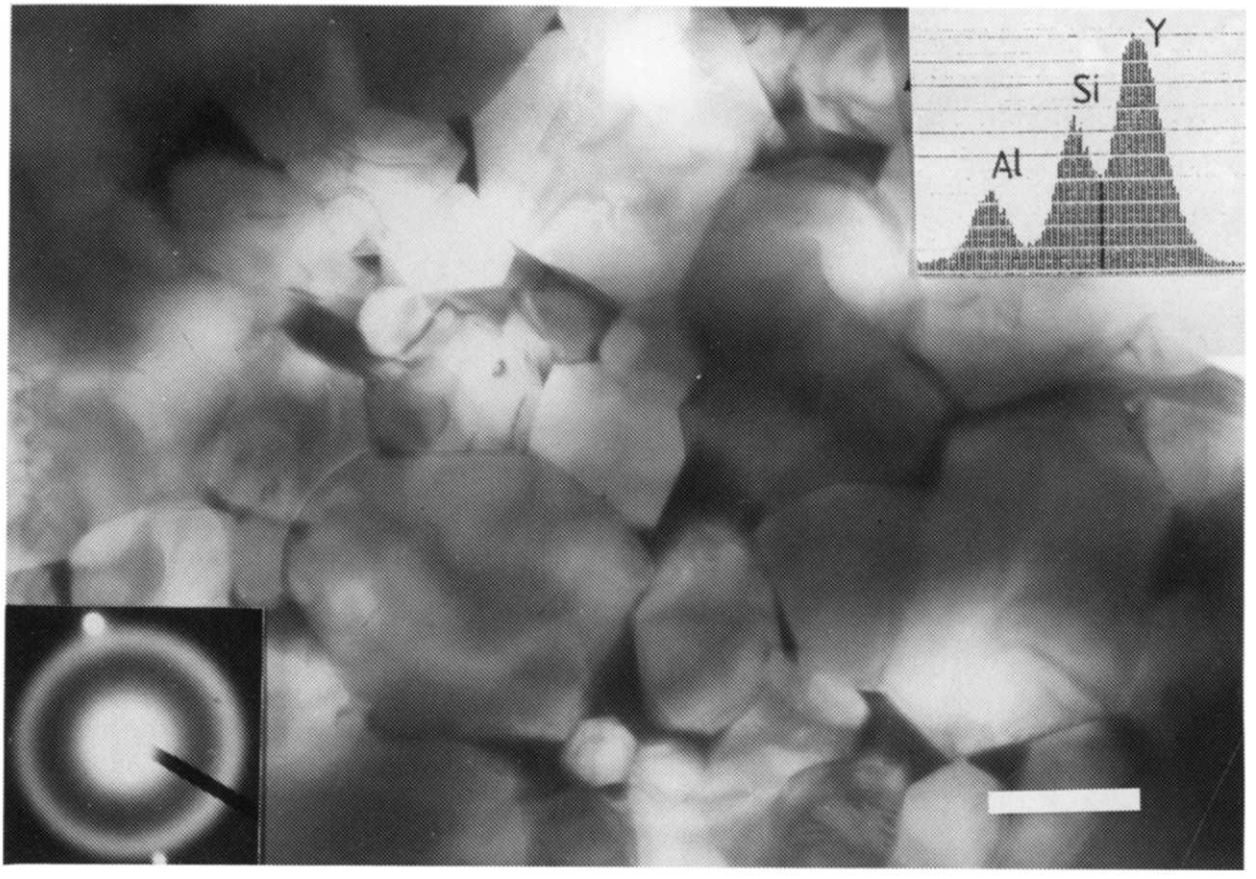

Fig. 5. TEM micrograph of sample A. The bar is 2·5 μm.

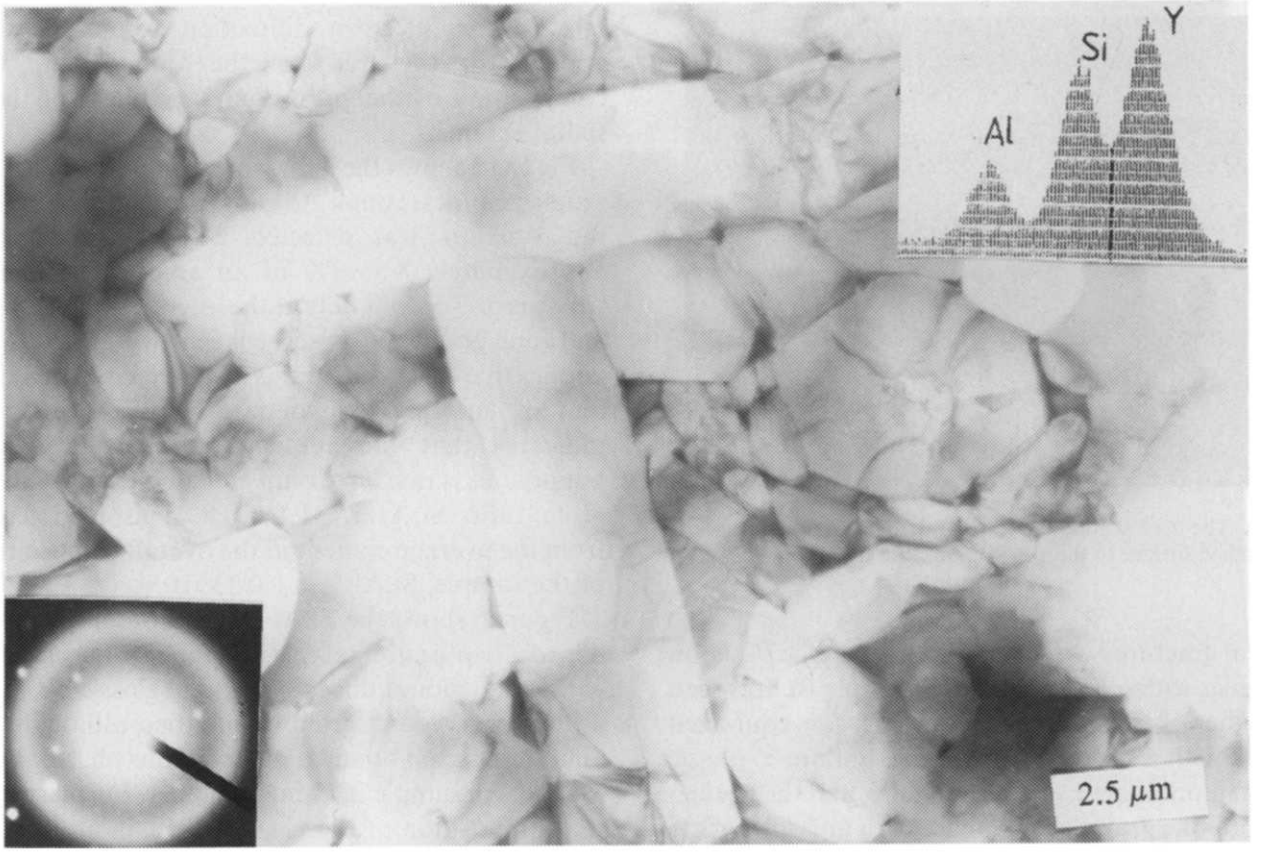

Fig. 6. TEM micrograph of sample B. The bar is 2·5 μm.

here only a very thin glassy film is present between two grains.

It is seen that the amount of glassy phase at grain boundaries is slightly increased with the increased amount of alumina in the mixtures, both in the case of α'- and mixed $\alpha' + \beta'$-sialon ceramics.

The TEM micrograph and the grain boundary composition of sample E are shown in Fig. 7. As pointed out above, the addition of the extra sintering additive La_2O_3 results in a fine grained microstructure. It is also seen, here, that the addition of La_2O_3 promotes the incorporation of yttrium into the lattice of the α'-phase while the composition of the grain boundary phase was changed to Si:Al:Y:La = 1:0·4:0·6:1·2, whereas the overall composition is Si:Al:Y:La = 1:0·23:0·05:0·003. However, the amount of glassy phase at grain boundaries is greatly increased to about 16 vol%, almost doubled compared with Sample A.

High resolution TEM imaging reveals that there are many crystal defects in the α'-grains in sample E, as shown in Fig. 8, which are hardly found in samples without La_2O_3 in the starting mixtures. However, it was not possible to detect the presence of La^{3+} ions in the crystal lattice of α'-sialons, showing that the solubility, if any, is very low.

5 Discussion

Up to now, the basic quantitative understanding of the microstructural development in Si_3N_4 and sialon is unsatisfactory. Therefore, the emphasis in this work was placed on observing the microstructural changes depending on the composition of the starting materials and interpreting the results only qualitatively. The experimental results indicate that the addition of oxides as either structural modifiers or extra sintering additives to the starting mixtures exhibits evident influences on the microstructures of both monolithic and composite $\alpha' + \beta'$-sialon ceramics.

For α'-sialon ceramics, the authors have shown elsewhere[8] that the alumina powder used in the starting mixtures reacts with yttria to form $3Y_2O_3 . 5Al_2O_3$ at moderate temperatures and then dissolves into the liquid at temperatures above 1600°C. This reduces the amount of the liquid phase at low temperatures, but results in the formation of a large amount of oxygen-rich liquid phase above 1600°C. Therefore, grain growth is suppressed in the beginning, but proceeds faster at higher temperatures when the viscosity of the liquid is low. As a result, however, the grain sizes of the final products are almost the same. Figure 9 shows this behaviour. A similar reaction sequence was observed in the case of mixed $\alpha' + \beta'$-sialons. The growth of α'-grains is almost identical with that in monolithic α'-sialon ceramics; however, the variation of the quantity and viscosity of the liquid phase was seen to influence the grain growth of β'-sialons.[14] It was observed earlier for liquid phase sintering of silicon nitride[15] that a high viscosity of the liquid phase leads to a slow reduction of the supersaturation and a higher aspect ratio. The authors' observation that the aspect ratio of β'-sialon grains decreases strongly with increasing amount of alumina is in conformity with this. This influence of the degree of supersaturation indicates that there are different growth mechanisms for the basal and prism planes.

According to the phase diagrams,[7,16,17] the yttria and alumina used in the starting mixtures are totally soluble in the structures of α'- and β'-sialons. However, the experimental results show that only a part of the oxides was incorporated into the crystal lattice of the final products, while the other part was consumed to form an amorphous phase remaining at grain boundaries. In general, it is seen that the increasing amount of oxides (yttria and/or alumina) results in an increasing amount of grain boundary phase. The influence of the addition of La_2O_3 on the microstructure of α'-sialon ceramics is significant. First, the grain size of the α'-phase is largely reduced, which can be explained due to the large amount of liquid phase formed during sintering. The authors have shown by dilatometry that shrinkage in the lanthanum oxide-doped samples starts as early as at 1200°C and reaches a first maximum at about 1400°C. In the samples without lanthanum oxide, shrinkage starts only above 1300°C and reaches a first maximum rate at about 1500°C. This clearly shows the importance of the liquid formation. The large amount of a low viscosity liquid phase results in a low supersaturation and fine, equi-axed grains. Secondly, the addition of La_2O_3 promotes incorporation of yttrium cations into the crystal lattice of α'-sialons. This can be expected since the distribution coefficient for the larger La^{3+} ions will be smaller than for the Y^{3+} ions. However, as a result of the formation of a large amount of an oxygen-rich liquid phase, a large amount is formed of an amorphous phase remaining at grain boundaries. Thirdly, the La_2O_3 addition leads to the formation of crystal defects in the α'-sialon lattice. Although it was generally accepted that Ce^{3+} and La^{3+} cations cannot be incorporated into the lattice of α'-sialons due to their large size, recent reports have shown that Ce^{3+} together with Y^{3+} can enter the crystal lattice, resulting in the formation of a lot of crystal defects.[12,13] The authors' observation of a large number of crystal defects in the La-doped samples, which are not present in samples without La, indicates in the same direction. However, the amount of La in the crystals is too low to be detected

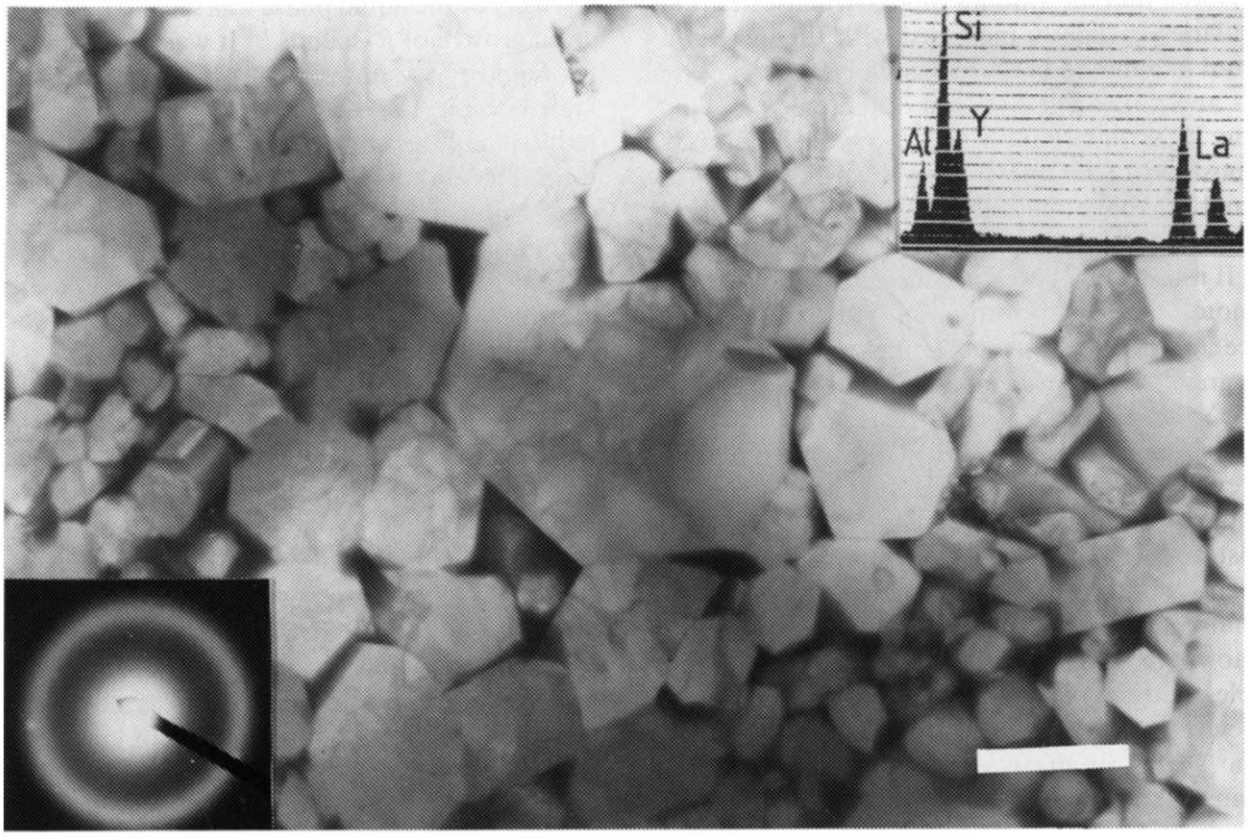

Fig. 7. TEM micrograph of sample E. The bar is 2·5 μm.

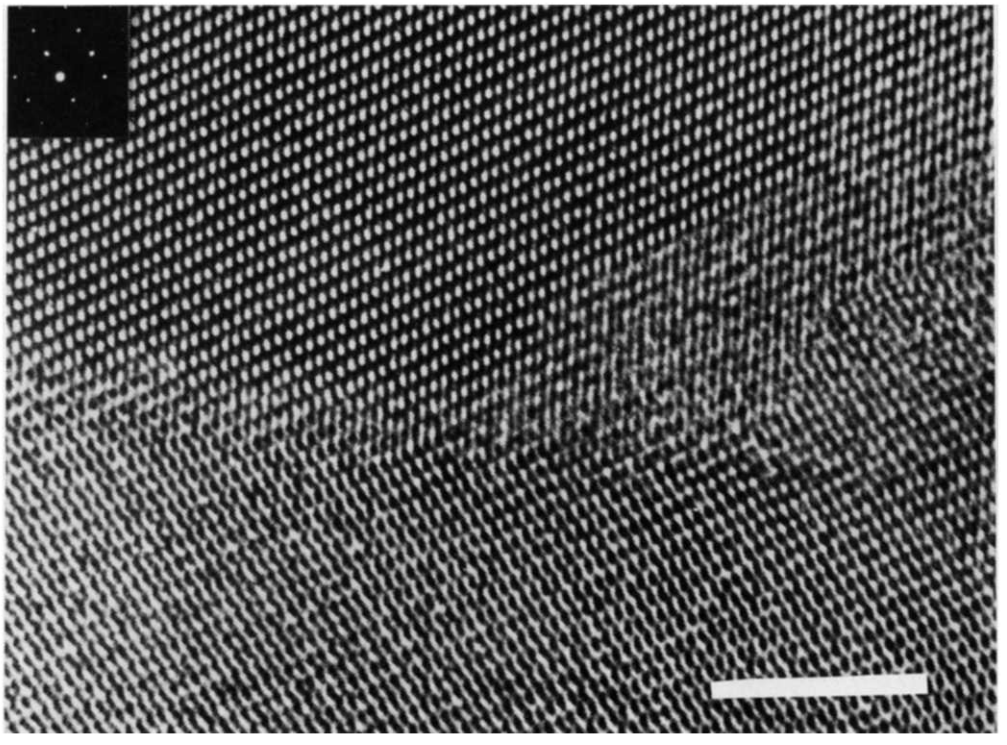

Fig. 8. High resolution TEM image of a type of crystal defects in sample E. The bar is 5 nm.

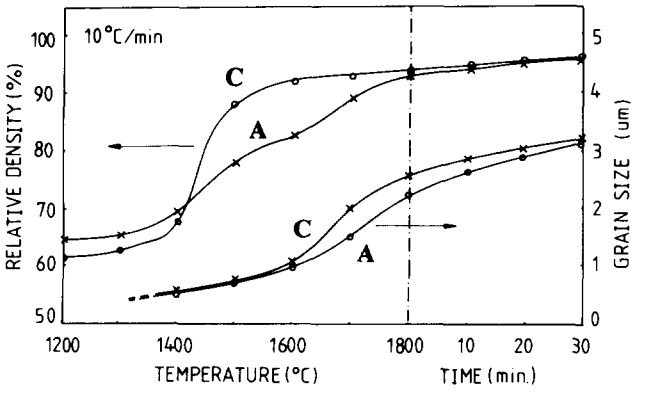

Fig. 9. Relative density and mean grain size for samples A and C. Heating rate 10°C/min, followed by 30 min at 1800°C.

by EDS. To prove this hypothesis more detailed work is necessary. Also, the mechanism of the defect formation and the type of defects remains unclear.

The oxygen impurity present in both silicon nitride (about 1·57 wt%) and aluminium nitride (about 1·80 wt%) has not been taken into account in the discussion above, but can nevertheless exhibit an influence on the microstructure of the final products. Qualitative considerations may lead to the changes which follow. In general, the oxygen impurity in nitrides is considered to be in the form of oxides, i.e. silica or silicon oxynitride in silicon nitride and alumina in aluminium nitride. At high temperatures these oxides will react with nitrides to form β'-sialons in the following reactions:[18]

$$Si_3N_4 + SiO_2{:}2AlN \rightarrow \beta'\text{-sialon} \quad (1)$$

$$Si_3N_4 + Al_2O_3{:}AlN \rightarrow \beta'\text{-sialon} \quad (2)$$

As a consequence, for example, composite $\alpha' + \beta'$-sialons were obtained in the surface layer of the sintered sample C, although monolithic α'-sialon was expected according to the phase diagrams.[7,16,17]

In a similar way, the oxides also can enter the lattice of α'-sialons by reacting with yttria and nitrides:

$$Si_3N_4 + AlN + Y_2O_3 + SiO_2 + Al_2O_3 \rightarrow \alpha'\text{-sialons} \quad (3)$$

Therefore, an overall composition shift of sialons composition towards the oxygen-rich side is expected. Additionally, the oxygen impurities present in the nitrides were also found to increase the amount of the amorphous grain boundary phase.

6 Summary

It is seen that the typical microstructure of α'- and mixed $\alpha' + \beta'$-sialon ceramics consists of crystalline phases of sialons and a small amount of amorphous phase remaining at grain boundaries; no other secondary crystal phase was found.

Increasing amounts of oxides both of structural modifiers and extra sintering additives in the starting mixtures are found to increase the amount of the amorphous grain boundary phase. The oxygen impurities not only change the overall composition of the sialons, but also result in an increasing amount of glassy grain boundary phase.

α'- and $\alpha' + \beta'$-sialon materials show differences in microstructure. While α'-sialons are characterized by equi-axial grains, the $\alpha' + \beta'$ materials consist of equi-axial α'-phase and needle- or fibre-like grains of the β'-phase.

It has been found that the addition of alumina to the starting mixtures decreases the aspect of β'-grains, but has very little influence on the grain size of the α'-phase. In contrast, the addition of La_2O_3 leads to fine grained α'-sialon ceramics.

Although La^{3+} ions are too large to be incorporated into the structure of α'-sialons, there are indications that some La^{3+} ions together with small ions like Y^{3+} can enter the lattice of α'-sialons, resulting in the formation of crystal defects.

Acknowledgements

The authors gratefully acknowledge Ing. J. P. G. M. van Eijk for his technical support and Mr J. W. Feng, Shanghai Institute of Ceramics, for his cooperation on the TEM observation.

References

1. Jack, K. H., In *Progress in Nitrogen Ceramics*, ed. F. L. Riley. NATO SAI Series E65. Martinus Nijhoff, The Hague, 1983, p. 45.
2. Jack, K. H., In *Non-oxide Technical and Engineering Ceramics*, ed. S. Hampshire. Elsevier Applied Sciences, Amsterdam, 1986, p. 1.
3. Cao, G. Z. & Metselaar, R., *Chem. Mater.*, **3** (1991) 242.
4. Jasper, C. A. & Lewis, M. H., *4th Int. Symp. Ceramic Materials and Components for Engines*, June 1991, Gothenburg, ed. R. Carlsson. Elsevier Appl. Sci., London, 1992, pp. 188–95.
5. Cao, G. Z., Metselaar, R. & Ziegler, G., In *Euro-Ceramics I*, ed. G. de With, R. A. Terpstra & R. Metselaar. Elsevier Applied Science, Amsterdam, 1989, p. 1.346.
6. Bartek, A., Ekström, T., Herbertsson, H. & Johansson, T., *J. Amer. Ceram. Soc.*, **75** (1992) 432.
7. Stutz, D., Greil, P. & Petzow, G., *J. Mater. Sci.*, **5** (1986) 335.
8. Cao, G. Z., Metselaar, R. & Ziegler, G., In *Ceramics Today—Tomorrow's Ceramics, Mat. Sci. Monographes 66B*, ed. P. Vincenzini. Elsevier, Amsterdam, 1991, p. 1285.
9. Ueno, K. & Toibana, T., *Yogyo*-Kyokai-*Shi*, **91** (1983) 409.
10. Xu, Y. R., Huang, L. P., Fu, X. R. & Yan, D. S., *Sci. Sin.*, **A28** (1985) 556.
11. Söderlund, E. & Ekström, T., *J. Mater. Sci.*, **25** (1990) 4815.
12. Olsson, P.-O., *J. Mater. Sci.*, **24** (1989) 3878.
13. Ekström, T., Jansson, K., Olsson, P.-O. & Persson. *J. Eur. Ceram. Soc.*, **8** (1991) 3.
14. Cao, G. Z., Preparation and characterization of α'-sialon ceramics. PhD, thesis, Eindhoven University of Technology, Eindhoven, 1991.

15. Wötting, G., Kanka, B. & Ziegler, G., In *Non-oxide Technical and Engineering Ceramics*, ed. S. Hampshire. Elsevier Applied Sciences, Amsterdam, 1986, p. 83.
16. Huang, Z. K., Greil, P. & Petzow, G., *J. Amer. Ceram. Soc.*, **66** (1983) C96.
17. Slasor, S. & Thompson, D. P., *J. Mater. Sci. Lett.*, **6** (1987) 315.
18. Ukyo, Y. & Wada, S., In *Euro-Ceramics I*, ed. G. de With, R. A. Terpstra & R. Metselaar. Elsevier Applied Science, Amsterdam, 1989, p. 1.566.